

Is there seismic attenuation in the mantle?

Y. Ricard^a, S. Durand^a, J-P. Montagner^b, F. Chambat^a

^a*Laboratoire de Géologie de Lyon - Terre Planète Environnement, CNRS UMR5570, École Normale Supérieure de Lyon, Université de Lyon, Université Claude Bernard Lyon 1, 46 Allée d'Italie, 69364 Lyon Cedex 07, France*

^b*Institut de Physique du Globe de Paris, Université Paris-Diderot, 1 rue Jussieu, 75238 Paris Cedex 05, France*

Abstract

The small scale heterogeneity of the mantle is mostly due to the mixing of petrological heterogeneities by a smooth but chaotic convection and should consist in a laminated structure (marble cake) with a power spectrum $S(k)$ varying as $1/k$, where k is the wavenumber of the anomalies. This distribution of heterogeneities during convective stirring with negligible diffusion, called Batchelor regime is documented by fluid dynamic experiments and corresponds to what can be inferred from geochemistry and seismic tomography. This laminated structure imposes density, seismic velocity and potentially, anisotropic heterogeneities with similar $1/k$ spectra. A seismic wave of wavenumber k_0 crossing such a medium is partly reflected by the heterogeneities and we show that the scattered energy is proportional to $k_0 S(2k_0)$. The reduction of energy for the propagating wave appears therefore equivalent to a quality factor $1/Q \propto k_0 S(2k_0)$. With the specific $1/k$ spectrum of the mantle, the resulting apparent attenuation should therefore be frequency independent. We show that the total contribution of 6-9% RMS density, velocity and anisotropy would explain the observed S and P attenuation of the mantle. Although these values are large, they are not unreasonable and we discuss how they depend on the range of frequencies over which the attenuation is explained. If such a level of heterogeneity were present, most of the attenuation of the Earth would be due to small scale scattering by laminations, not by intrinsic dissipation. Intrinsic dissipation must certainly exist but might correspond to a larger, yet unobserved Q . This provocative result would explain the very weak frequency dependence of the attenuation, and the fact that bulk attenuation seems negligible, two observations that have been difficult

to explain for 50 years.

Keywords: Apparent attenuation, Q, scattering, random media

*Corresponding author. Tel: +33 (0)4 72 44 84 13 *E-mail address:* ricard@ens-lyon.fr (Y. Ricard)

1. Introduction

After reviewing laboratory and seismological observations, Knopoff (1964) concluded that the seismic quality factor Q (or attenuation Q^{-1}) depended only weakly on the frequency ω . This observation was not easily compatible with the theoretical models developed for the anelastic behavior. Indeed, these models predicted a frequency dependent behavior with a maximum of absorption centered on a frequency related to the relaxation time of a given mechanism. Later, Jackson and Anderson (1970) and Liu et al. (1976) proposed to explain this quasi frequency-independent behavior by the superposition of standard linear solids whose relaxation times covered the observed absorption band.

In the last 30 years, seismological studies have however identified some frequency dependence of the attenuation. From normal modes and surface waves (say in the range 0.001-0.05 Hz), a weak dependence of the attenuation has been proposed with $Q^{-1} \propto \omega^\alpha$ and $\alpha \approx -0.2$ (e.g., Lekic et al., 2009). An exponent in the same range ($-0.4 \leq \alpha \leq 0$) has been found using body waves up to ≈ 1 Hz (e.g., Choy and Cormier, 1986; Shito et al., 2004). Somewhere above 1 Hz there is strong evidence of a corner past which the exponent becomes closer to $\alpha \approx -1$ (Choy and Cormier, 1986; Cormier, 2011). On the low frequency side, below 0.001 Hz, the attenuation is likely increasing moderately with $\alpha \approx 0.4$ (Lekic et al., 2009). Within a large frequency domain, 10^{-4} -1 Hz, the attenuation varies therefore by less than an order of magnitude.

A modest frequency dependence of the attenuation ($\alpha \approx -0.27$) has also been observed in laboratory experiments with polycrystalline aggregates of olivine (Jackson et al., 2002; Faul and Jackson, 2005). The similarity of exponents found in laboratory experiments and in seismological observations suggests that similar dissipation mechanisms might be present in the two situations. The laboratory experiments are however performed under conditions that are not identical to the seismologic situation (viscoelastic torsion rather than seismic propagation, smaller material grain sizes, larger strain rates, much smaller scale...). Several possible micromechanisms of attenuation have been suggested (see Jackson, 2007, for a review); it is only by a specific combinations of them, distributed over a large attenuation

29 band that the seismic observations can be accounted for.

30 The attenuation in the mantle seems to be mostly due to shear attenuation Q_μ^{-1} (μ is
31 rigidity) while bulk attenuation Q_κ^{-1} (κ is incompressibility) is much smaller (e.g., Romanow-
32 icz and Mitchell, 2006). This behavior is surprising for the following reason. Submitting an
33 elastic medium to extension results in a perpendicular deformation generally in compression
34 and controlled by a positive Poisson's ratio $\nu = (3\kappa - 2\mu)/(6\kappa + 2\mu)$. Therefore, for most
35 materials, $3\kappa > 2\mu$ (this is not a thermodynamic rule but simply an empirical observa-
36 tion; some rare materials called auxetic have a negative Poisson's ratio). For a dissipative
37 medium submitted to a slow stretching, one would also expect the perpendicular velocity
38 to be similarly in compression. For a linear solid, the correspondence principle relates the
39 velocities to the deformations by replacing the real elastic parameters κ and μ by their
40 imaginary counterparts κQ_κ^{-1} and μQ_μ^{-1} . Therefore one would expect $3\kappa Q_\kappa^{-1} > 2\mu Q_\mu^{-1}$ or
41 $Q_\kappa^{-1} > (2\mu)/(3\kappa)Q_\mu^{-1}$ (Morozov, 2013); a Q_κ^{-1} of order $0.2 Q_\mu^{-1}$ or larger would be expected
42 rather than the surprising $Q_\kappa^{-1} \approx 0$.

43 The attenuation measured by seismologists is in fact a combination of various mecha-
44 nisms. Some are really dissipative (i.e., they convert the elastic energy into heat), some are
45 due to various non-dissipative effects (i.e., the coherent elastic energy is refracted, scattered
46 into incoherent signals, defocused...). In the latter case, the coherent elastic energy is lost for
47 a direct observation but remains distributed in the Earth (before being eventually dissipated
48 in the fluid and solid envelopes of the Earth). This "elastic" attenuation is hard to quantify
49 and makes the measurements of intrinsic attenuation difficult for body waves and surface
50 waves (see review by Romanowicz and Mitchell, 2006; Shearer and Earle, 2008). Attenuation
51 can also be derived with normal modes from the width of spectral peaks (Dahlen, 1982).
52 Mode coupling by heterogeneities broadens the spectral peaks and again, separating this
53 effect from intrinsic attenuation is complex. A similar difficulty for separating intrinsic and
54 extrinsic phenomena exists also for anisotropy (Wang et al., 2013; Fichtner et al., 2013).

55 In this paper we will estimate the elastic attenuation that can be due to the hetero-
56 geneities in density, velocity or anisotropy of the mantle. We show that the specific spec-
57 trum of the heterogeneities in the mantle implies, as it is observed, that the P and S elastic

58 attenuations should be frequency independent and that the P attenuation should be likely
59 smaller than the S attenuation. These attenuations interpreted in terms of Q_κ , Q_μ agree
60 with $Q_\kappa \gg Q_\mu$ without implying a surprising auxetic rheology for the mantle. In order
61 to reach the typical observations of attenuation in the mantle, heterogeneities of 6-9 % in
62 density, velocity and anisotropy are needed. These values are very large but might not be
63 unreasonable. For a lower level of heterogeneities, intrinsic attenuation would dominate a
64 frequency independent elastic attenuation.

65 **2. Heterogeneities in the mantle**

66 The smooth large scale heterogeneities of the mantle are likely due to lateral temperature
67 variations related to thermal convection. However at small length scale there are more
68 certainly related to petrological/compositional anomalies. As thermal diffusivity is much
69 larger than chemical diffusivity, the gradients of composition remain indeed much sharper
70 than those of temperature. Compositional heterogeneities, like thermal ones, induce density,
71 velocity but also anisotropy variations. The origin of compositional variations in the mantle
72 could be due to a primordial layering of the mantle and more obviously to the continuous
73 injection of oceanic lithosphere in the mantle (Coltice and Ricard, 1999). The difference
74 in density or velocity between oceanic crust and depleted harzburgite reaches 10% and
75 although these two components undergo various phase changes when the lithospheric slab
76 sinks in the mantle, contrasts of several % should remain throughout the mantle (Ricard et
77 al., 2005). The presence of localized melt bands (in the upper mantle at least), with 5%
78 or more impedance contrasts has also been observed (Kawakatsu et al., 2011; Tauzin et al.,
79 2010).

80 The mixing of heterogeneities in chaotic convecting fluids has been studied for a long
81 time. In situations appropriate for the Earth, when heterogeneities are continuously injected
82 on a length scale smaller than that of a flow which is smooth but chaotic, the heterogeneity
83 power spectrum should vary like $1/k$ where k is the wavenumber of the heterogeneity ($k =$
84 $2\pi/\lambda$ where λ is the wavelength). This result was obtained by Batchelor (1959) and is
85 sometimes called "Batchelor rule". These steady state results have been extended and

86 confirmed for initial value problems (Antonsen and Ott, 1991). The basic physics that leads
87 to this result is rather simple to explain (Olson et al., 1984). The homogeneization in the
88 mantle does not occur by diffusing away the heterogeneities but rather by stirring them.
89 Advected by the flow, a heterogeneity of wavelength λ , is stretched and folded (the so-call
90 "baker" transformation, where the pastry maker kneads the dough is prototypical of a mixing
91 process). A heterogeneity is therefore transformed into a thin sheet mutiply folded. This
92 process continuously reduces the wavelength of the heterogeneities and the energy cascades
93 down the power spectrum toward the large wavenumbers. The injection replenishes the low
94 wavenumber spectrum and in steady state, a $1/k$ spectrum results.

95 Several authors have tried to infer the power spectrum of the mantle from geochemical or
96 seismic observations. From isotopic Sr variations of ridge basalts, Gurnis (1986) suggested
97 that the power spectrum of the mantle may be rather flat ("white") which would imply
98 a drastic heterogeneity at short wavelength. Using a similar approach but with orders of
99 magnitude more data and several isotopic ratios, Agranier et al. (2005) observed a clear $1/k$
100 spectrum along much of the Atlantic ridge.

101 Long wavelength tomography probably maps thermal heterogeneity that may decrease
102 faster than a $1/k$ spectrum (Montagner, 1994). However this decrease is partially due to
103 the regularization of the inversion (Ricard et al., 1996) and a spectrum closer to $1/k$ is also
104 obtained by patching together global and regional tomographies (Chevrot et al., 1998). A
105 more precise estimate of the short wavelength content of the mantle comes from fitting the
106 amplitude of PKP precursors in the mantle. Following the pioneering works of Cormier
107 (1995) and Hedlin et al. (1997), a study by Margerin and Nolet (2003) found small RMS
108 P velocity (0.1-0.2%) in the deep Earth. This low level of short wavelength (≈ 10 km)
109 heterogeneities has been recently confirmed by Mancinelli and Shearer (2013).

110 The view that emerges from our understanding of mantle stirring, of plate tectonics,
111 from observations of geochemical heterogeneities and of small scale seismic observations
112 is therefore in agreement with a "marble cake" mantle structure as advocated by Allègre
113 and Turcotte (1986). The mantle should consist of a laminated medium with low velocity
114 contrasts between layers and a power spectrum decreasing as $1/k$. We want now to compute

115 how much seismic energy could be lost by scattering in such a medium.

116 **3. Apparent attenuation of a seismic S wave propagating in a laminated struc-** 117 **ture**

118 To illustrate the potential effect of small scale heterogeneities on the amplitude of a
119 wave, we consider the simple case of a seismic S wave propagating perpendicularly along
120 z (polarized in the xy plane) through layers of different properties. We will discuss the
121 case of a P wave, of anisotropy and of non-perpendicular incidences later. The rigidity
122 $\mu(z)$, or density $\rho(z)$ are only functions of z . An upgoing wave, incident on $z = 0$, with
123 amplitude $(S_{ux}(0), S_{uy}(0))^t$ is partly reflected by the laminations as a downgoing wave of
124 amplitude $(S_{dx}(0), S_{dy}(0))^t$ and partly transmitted at the distance z as a wave of amplitude
125 $(S_{ux}(z), S_{uy}(z))^t$. Transmission T_u and reflection R_u matrices for the upward propagation
126 can be defined as

$$\begin{pmatrix} S_{ux}(z) \\ S_{uy}(z) \end{pmatrix} = T_u \begin{pmatrix} S_{ux}(0) \\ S_{uy}(0) \end{pmatrix} \quad (1)$$

127 and

$$\begin{pmatrix} S_{dx}(0) \\ S_{dy}(0) \end{pmatrix} = R_u \begin{pmatrix} S_{ux}(0) \\ S_{uy}(0) \end{pmatrix} = R_u T_u^{-1} \begin{pmatrix} S_{ux}(z) \\ S_{uy}(z) \end{pmatrix}. \quad (2)$$

128 An incident wave of unit amplitude polarized on the x axis and propagating in such a stack
129 of anisotropic layers will give rise to two reflected waves polarized on both x and y axis,
130 $R_{u_{xx}}$ and $R_{u_{xy}}$, and two transmitted waves, $T_{u_{xx}}$ and $T_{u_{xy}}$. In an isotropic R_u and T_u are
131 diagonal.

132 Of course if the structure of the propagating medium were perfectly known, the changes
133 in amplitude of the propagating wave and the existence of a back propagating wave will be
134 correctly interpreted as a purely conservative phenomenon (without dissipation). However if
135 the structure is not accurately known, the change in amplitude of the wave will likely be in-
136 terpreted as attenuation (scattering attenuation). We will define the equivalent attenuation
137 for a seismic wave with wavenumber k_0 in our laminated medium as (for the x -polarization)

$$\frac{S_{ux}(k_0, z)}{S_{ux}(k_0, 0)} = T_{u_{xx}} = \exp\left(-\frac{k_0 z}{2Q(k_0)}\right). \quad (3)$$

138 For each wavenumber k_0 , an attenuation $Q(k_0)^{-1}$ can therefore be computed.

139 To obtain the reflection and transmission matrices of a complex medium, we use a method
 140 related to the "O'Doherty-Anstey" approach (O'Doherty and Anstey, 1971) and discussed
 141 in Shapiro et al. (1996). We start from the wave propagation equation transformed in such a
 142 way to construct the differential system verified by the transmission and reflection matrices
 143 (see supplementary material A and the differential system (A.12)). This system solved
 144 by a standard Runge-Kutta algorithm allows the exact computation of the reflection and
 145 transmission properties. Our results have been checked to be identical to those computed
 146 by a transfer matrix scheme akin to the Thomson-Haskell method.

147 The advantage of the O'Doherty-Anstey approach to the Thomson-Haskell method is
 148 that we can identify the average propagation (in a homogeneous equivalent isotropic medium
 149 with rigidity μ_0 and density ρ_0) and the effects of the perturbations due to the variations of
 150 rigidity and density along the ray. Assuming that all these perturbations $\delta\mu/\mu$ and $\delta\rho/\rho_0$
 151 are small we can derive an analytical estimate of the exact solution by Taylor expansion (see
 152 (A.14)). The main result of this cumbersome analytical work is very simple. The equivalent
 153 attenuation seen by the wave is simply

$$\frac{1}{Q} = \frac{\sqrt{2\pi}}{4} k_0 S_S(2k_0) \quad (4)$$

154 where S_S is the power spectrum of the quantity.

$$\frac{\delta\mu}{\mu} + \frac{\delta\rho}{\rho_0}, \quad (5)$$

155 (the formalism involves $\delta\rho/\rho_0 = (\rho(z) - \rho_0)/\rho_0$ and $(\mu_0^{-1} - \mu(z)^{-1})/\mu_0^{-1} = (\mu(z) - \mu_0)/\mu_0 =$
 156 $\delta\mu/\mu$). The same approach can be used with P waves (see supplementary material B). Not
 157 surprisingly, we obtain an equivalent attenuation similar to (4) but where the spectrum S_S
 158 (5) is replaced by the spectrum S_P that also involves incompressibility K ,

$$\frac{\delta(K + 4\mu/3)}{K + 4\mu/3} + \frac{\delta\rho}{\rho_0}. \quad (6)$$

159 This implies that the knowledge of the spectra of heterogeneities in elastic parameters,
 160 density and (see later) anisotropy, allows the estimate of the scattering attenuation of the
 161 medium.

162 We assume in this paper that the elastic parameters have small amplitude variations;
 163 classically the assumption of effective medium (Backus, 1962; Capdeville and Marigo, 2007)
 164 is that the sizes of the heterogeneities are small compared to the wavelength of the seis-
 165 mic wave. The two approaches share however the same mathematical tools (perturbation
 166 formalism) and the same physical goals (averaging the perturbations). Notice also that
 167 the average equivalent properties of a laminated medium can be obtained numerically by a
 168 composite elastic medium theory (Kaelin and Johnson, 1998). It seems however uneasy with
 169 this formalism to relate analytically the spectrum of the heterogeneities to the apparent
 170 attenuation.

171 4. Examples of "elastic" attenuation

172 To test the quality of our analytical estimate of the attenuation (4), let us consider the
 173 propagation of an elastic wave crossing a 1D medium made of layers of identical thicknesses
 174 h . In each layer the elastic parameters are uniform, isotropic, but the density is $\rho_0 + \delta\rho(z)$
 175 where $\delta\rho$ is a small perturbation (this applies to both S or P waves, see (5) and (6)). We
 176 assume that $\delta\rho/\rho_0$ is a random variable uniformly distributed over $[-r, r]$. Such a medium
 177 is described in Figure (1a) where we have chosen $r = \sqrt{3}/100$ so that the RMS of $\delta\rho/\rho_0$, σ
 178 is 1%.

179 The autocorrelation $R(z)$ of such a medium (see definition (A.27)) can be easily found
 180 in the limit of an infinite medium

$$\begin{aligned}
 R(z) &= \sigma^2 \left(1 - \frac{|z|}{h}\right) \quad \text{for } |z| < h \\
 R(z) &= 0 \quad \text{for } |z| > h.
 \end{aligned}
 \tag{7}$$

181 The exact autocorrelation of the function shown in Figure (1a) is plotted in Figure (1b)
 182 with a black line, and its approximation according to (7) with a red line.

183 The Wiener-Khinchin theorem (A.28) relates the autocorrelation $R(z)$ to the power spec-
 184 trum $S(k)$ of the medium

$$S(k) = \frac{1}{\sqrt{2\pi}} \int_{-\infty}^{+\infty} R(z) e^{-ikz} dz = \frac{4\sigma^2}{\sqrt{2\pi}} \frac{\sin^2(kh/2)}{k^2h}.
 \tag{8}$$

185 The power spectrum of the function depicted in Figure (1a) and that given by (8) are shown
 186 in Figure (1c) (black and red lines).

187 The expression (4) (in which $S_S = S = S_P$) indicates therefore that the elastic attenua-
 188 tion is of order

$$\frac{1}{Q} = \frac{\sqrt{2\pi}}{4} k_0 S(2k_0) = \frac{\sigma^2 \sin^2(k_0 h)}{4 k_0 h} \quad (9)$$

189 In Figure (1d) we depict this expression as a function of k_0 , (red) and the exact elastic atten-
 190 uation $-2 \log(T_{dxx})/(k_0 z)$ (black) obtained by propagating a wave across the 1D structure
 191 of Figure (1a). The exact propagation has been computed using the equations (A.12) and
 192 with a modified Thomson-Haskell code, the computations give identical results for S and
 193 for P waves. We can also generate a series of random laminated structures and average the
 194 transmission coefficients. This is depicted by the green line of Figure (1d) which averages the
 195 attenuations of 50 random distributions (arithmetic average of Q^{-1}): the statistical distri-
 196 bution of attenuation is identical to the prediction. Although the exact transmission is more
 197 complex than that predicted by the approximate solution, it is obvious that we successfully
 198 captured the elastic attenuation of the structure.

199 A more meaningful exercise can be performed for a medium in which the density has a
 200 power spectrum in $1/k$ like what is expected in Earth's mantle. To do so, we first generate
 201 Fourier coefficients of the form $\sqrt{S_0/k} \exp(i\phi(k))$ where the phase $\phi(k)$ is a random variable
 202 uniformly distributed over $[0, 2\pi[$, S_0 a constant and where the wavenumber k is taken
 203 between k_{min} and k_{max} . Then, we perform an inverse Fourier transform of these coefficients.
 204 By construction, the power spectrum of the resulting function is S_0/k for $k_{min} \leq k \leq k_{max}$;
 205 it has a RMS σ , which according to Parseval's identity is $\sigma^2 = \sum_k S_0/k \approx S_0 \log(k_{max}/k_{min})$.
 206 The elastic attenuation (4) between the wavenumbers $k_{min}/2$ and $k_{max}/2$ can therefore be
 207 written as

$$\frac{1}{Q} = \frac{\sqrt{2\pi}}{8} S_0 = \frac{\sqrt{2\pi}}{8} \frac{\sigma^2}{\log(k_{max}/k_{min})} \quad (10)$$

208 where $1/Q$ is expressed as a function of the amplitude of the heterogeneity spectrum or as
 209 a function of the heterogeneity RMS. The function and its spectrum are depicted in Fig-
 210 ure 2, panels (a) and (c), where we have chosen a perturbation RMS of 1%. Considering

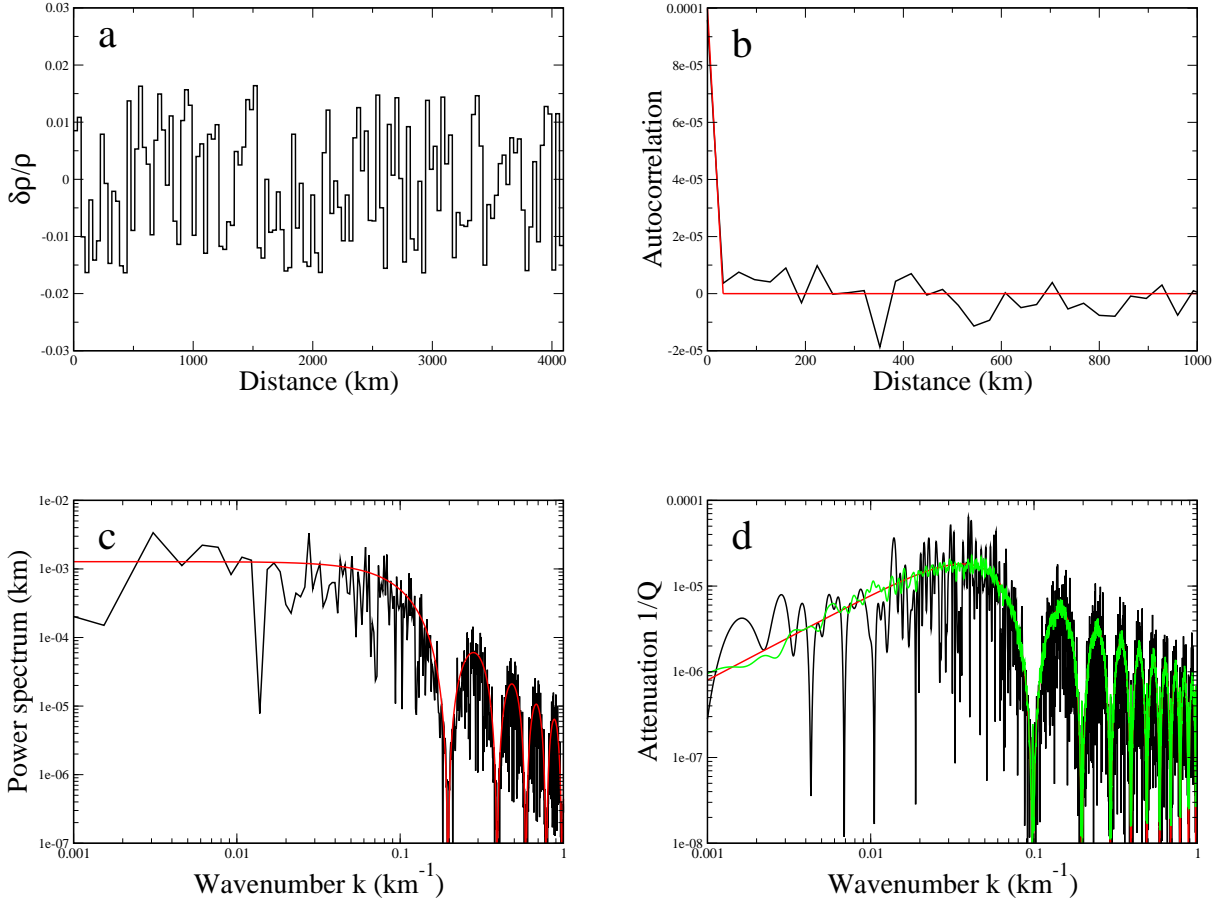


Figure 1: We generate a random density anomaly for a laminated structure. The laminations are 32 km thick. The density anomalies $\delta\rho/\rho_0$ have a RMS amplitude $\sigma = 1\%$ (panel a). The autocorrelation function of the density is statistically 0 except for distances smaller than h (black, panel b), the red line is the theoretical prediction (7). The power spectrum of the density and the prediction (8) are depicted by the black and red lines of panel (c). The first minimum would correspond to $k_0 = \pi/h$ or typically a period of a few seconds for a P wave. A wavenumber of 0.01 would correspond to a few 10 s. The apparent attenuation is shown in panel (d) (black) with the prediction (9) (red). The green attenuation corresponds to the average of 50 random realizations similar to that of panel (a). It confirms the theoretical prediction.

211 that Earth's attenuation is constant over 3-4 frequency decades, we choose $k_{max}/k_{min} =$
 212 $4096 = 10^{3.6}$. The autocorrelation function (panel b) is shown in black and the theoretical
 213 one (see A.28) in red (this function is a cosine integral). In the inserted panel we also use a

214 semilogarithmic scale to show that the autocorrelation is indeed very different from an expo-
 215 nential law (a straight line in semilogarithmic scale). The autocorrelation of heterogeneities
 216 in the Batchelor regime decreases much faster than the exponential at short distance but
 217 also maintains a significant correlation at long distance. According to (10), the equivalent
 218 attenuation (panel d, black) should be flat (wavenumber or frequency independent). This
 219 is the case and the analytical prediction (panel d, red) gives a good fit to the exact atten-
 220 uation. In green we average 50 random realizations similar to that of panel (a) to confirm
 221 the frequency independence of the elastic attenuation. Our analytical estimate seems how-
 222 ever to slightly underestimate the average attenuation (4×10^{-6} according to (10), instead of
 223 $\approx 5 \times 10^{-6}$; compare red and green curves in Figure 2d); this may be related to the choice
 224 of the averaging, here an arithmetic average of the Q^{-1} , geometric or harmonic averages
 225 of Q or Q^{-1} give different values also close to the analytical prediction in red). In Figure
 226 2, there are no units for the horizontal axis and for the power spectrum. There is indeed
 227 no characteristic length in this situation and only the ratio $k_{max}/k_{min} = 4096$ matters. If
 228 the distance in panel (a) is in a given *unit* (m, km...), then the wavenumbers are in $unit^{-1}$,
 229 the power spectrum in *unit* and the same amplitude of attenuation is recovered (but in a
 230 wavenumber range defined in $unit^{-1}$).

231 Although we only discussed the elastic attenuation, the propagation of seismic waves in
 232 this laminated mantle is also associated with dispersion; the effective propagation velocity
 233 is frequency dependent. Our approach implies that attenuation and dispersion are, as they
 234 should, related by the usual Kramers-Kronig relations (see A.20). Therefore, if our model
 235 is in agreement with the observed attenuation, it is also in agreement with the observed
 236 dispersion. For example, assuming a $1/k$ spectrum of the mantle implies both that the
 237 apparent attenuation $1/Q$ is a constant, and that the phase velocity $v(\omega)$ is frequency
 238 dependent with a dispersion deduced from (A.20), $1/v(\omega) = 1/v_0 - 2/(\pi Q) \log(\omega/\omega_0)$, which
 239 are two assumptions of Prem (Liu et al., 1976). Notice that the heterogeneity spectrum in
 240 $1/k$, which is in agreement with the attenuation and dispersion of Prem, is associated with
 241 an autocorrelation function (see Figure 2b) very different from an exponential which has
 242 been the hypothesis of several previous studies of mantle scattering.

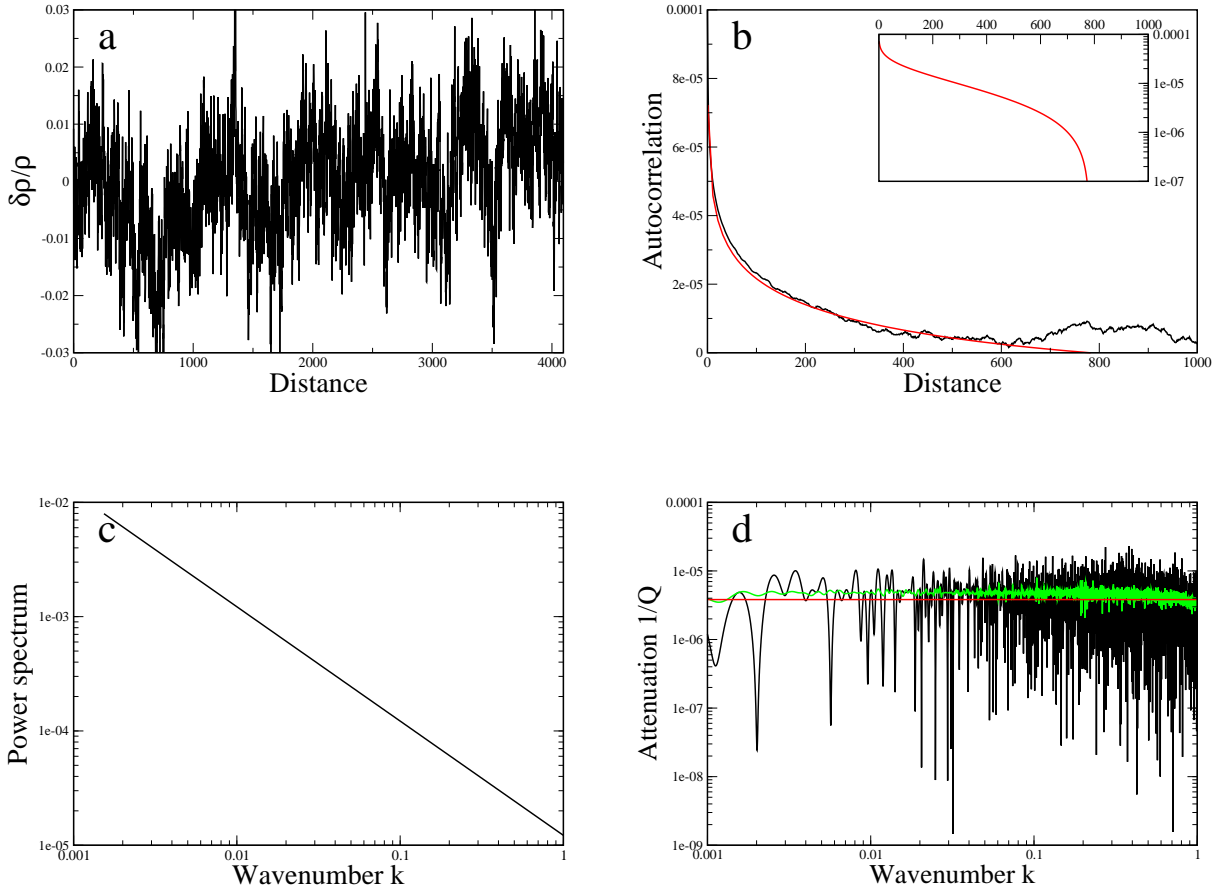


Figure 2: We generate a random density anomaly with power spectrum varying as $1/k$ in a range of wavenumbers covering 3.6 decades and with RMS 1% (panel a). The computed (black) and theoretical (red) autocorrelations are depicted in panel b. The inserted panel shows the theoretical autocorrelation curve in logarithmic scale to show that it is very different from an exponential (a straight line). The power spectrum is shown in panel c. The computed (black) and theoretical attenuation (red) are depicted in panel d. The green attenuation corresponds to the average of 50 random realizations similar to that of panel a.

243 5. Attenuation of the mantle

244 In the lower mantle Q_s^{-1} is found between $1/300$ (Prem) and $1/700$ (Hwang and Ritsema,
 245 2011; Durand et al, 2013) and Q_p^{-1} is of order $4/3(V_s/V_p)^2 Q_s^{-1}$ i.e., between $1/600$ and $1/1400$.
 246 This last relation results from the observation that the bulk attenuation Q_κ^{-1} is very low.
 247 In the upper mantle the attenuation is about twice larger than in the lower mantle. It

248 is tempting to compare these values to what can be estimated with our model of elastic
249 attenuation.

250 In Figure 2 we obtained $Q^{-1} \approx 5.10^{-6}$ for a 1% RMS density perturbation, assuming
251 that the medium is isotropic, with constant rigidity and with the same $1/k$ spectrum over a
252 wavenumber range of 3.6 decades. This range is the typical range of the seismic frequencies
253 over which the observed attenuation seems roughly constant. As this elastic attenuation
254 varies like the amplitude of $(\delta\rho/\rho_0)^2$ (see (10)), we would predict that 17% to 26% RMS
255 perturbations of density could explain the observed S attenuation in the lower mantle (12%
256 to 18% RMS perturbations for the P attenuation). These RMS values for the density are
257 certainly not reasonable for Earth's mantle anomalies. However, it is not only the density
258 but also the elastic parameters that influence the elastic attenuation.

259 In mineralogical models, (e.g., comparing the properties of basaltic crust and of normal
260 mantle at deep mantle conditions, as in Ricard et al. (2005)), the relative contrasts of elastic
261 parameters (assuming isotropy) have similar values that those of density and are generally
262 closely correlated. The power spectra of $\delta\mu/\mu + \delta\rho/\rho_0$ or of $\delta(K + 4\mu/3)/(K + 4\mu/3) + \delta\rho/\rho_0$
263 are therefore close to 4 times that of density alone (it would be 2 times for uncorrelated
264 variables with similar amplitudes). This would reduce the necessary perturbations needed
265 to explain the whole mantle attenuation by elastic attenuation only, by a factor 2 (i.e., 8-
266 13% density and elastic perturbations to explain the S attenuation, 6-9% to explain the P
267 attenuation).

268 In addition, anisotropy should be considered and in supplementary material (C) we
269 discuss the simple case of transverse anisotropy. Even in a medium where the density
270 and the isotropic velocity are uniform, the presence of anisotropy also induces an elastic
271 attenuation. The shear wave splitting leads to an apparent attenuation estimated from
272 pulse widths or spectra because of the arrival of two quasi-S waves in a window assumed
273 to contain a single S wave, when the period band of measurement is wider than the time
274 separation of the two pulses. This S attenuation is found to be related to the power spectra of
275 $\delta\mu/\mu + \delta\rho/\rho_0 + \delta a/\mu \cos(2\psi)$ and of $\delta a/\mu \sin(2\psi)$ where $a(z)$ is the amplitude of anisotropy
276 (difference between the two rigidities that characterizes the elasticity in this transverse

277 geometry) and $\psi(z)$ the direction of fast polarization in the xoy plane. Assuming that the
278 anisotropy direction is uncorrelated with ρ and μ , the S attenuation becomes related not
279 only to the power of $\delta\mu/\mu + \delta\rho/\rho_0$ but also of $\delta a/\mu$. Taking this effect into account reduces
280 the RMS amplitude of the density and elastic anisotropic parameters necessary to explain
281 both the P and S attenuations by elastic attenuation only, to around 6-9%.

282 In supplementary material D we also consider the case of a non normal incidence θ to the
283 lamination, in the simple case of a SH wave (so that S and P waves remain uncoupled). The
284 elastic attenuation is now a function of the incidence angle, and differs for density variations
285 and for elastic modulus variations. The situation is further complicated because complete
286 reflection can occur when $\theta \rightarrow \pi/2$. However when density and elasticity heterogeneities are
287 proportional, the final elastic attenuation (D.10) is independent of the incidence angle and
288 therefore identical to the case with normal incidence.

289 The P-SV case coupling P and S waves is much more cumbersome, but the same method
290 applies as shown in Shapiro et al. (1996). We do not include a supplementary section for
291 this case, as it would be even longer than the 4 supplementary sections already discussed.
292 Invariably we found that the attenuation of both P and SV waves are now dependent on
293 the combined spectra of density, rigidity and incompressibility, weighted by functions of
294 the incidence angle θ . Although we have not explored all the cases (the transmission and
295 coupling of a P and general S wave across a lamination with non-normal incidence), we are
296 confident that for a laminated medium with $1/k$ spectrum, the elastic attenuation remains
297 frequency independent and with a similar or larger (because the elastic energy can now be
298 exchanged between P and S waves) amplitude than with a normal incidence.

299 The heterogeneities needed to explain the Earth's attenuation by scattering only are
300 large. They are however comparable to what is proposed in the shallow mantle in terms
301 of lateral variations of density (from mineralogy, see Ricard et al. (2005)), seismic velocity
302 (e.g., Debayle and Ricard, 2012) or amplitude of anisotropy (e.g., Montagner and Guillot,
303 2002; Kawakatsu et al., 2011; Debayle and Ricard, 2013), and various localized reflectors
304 with large, positive or negative impedances are observed in the mantle (e.g., Schmandt et
305 al., 2011; Tauzin et al., 2010).

306 The large RMS heterogeneity that we estimate assumes that the same $1/k$ heterogeneity
 307 spectrum is valid across a wavenumber range of 3.6 decades. It is not directly comparable
 308 to the RMS heterogeneity estimates obtained for the lower mantle using high-frequency (\approx
 309 1 Hz) PKP precursors which only sample a limited number of wavelengths (Margerin and
 310 Nolet, 2003; Mancinelli and Shearer, 2013). To compare our model to these PKP precursor
 311 studies, we consider like in Mancinelli and Shearer (2013) that the small scale 1D structure
 312 has an exponential autocorrelation with a small correlation length $h = 6$ km. According to
 313 the Wiener-Khinchin theorem, (A.28) and the expression of $1/Q$, (4), the autocorrelation,
 314 the power spectrum and the elastic attenuation are

$$\begin{aligned}
 R(z) &= \sigma^2 \exp\left(-\frac{z}{h}\right) \\
 S(k) &= \frac{2\sigma^2}{\sqrt{2\pi}} \frac{h}{1 + k^2 h^2} \\
 \frac{1}{Q} &= \frac{\sigma^2}{2} \frac{kh}{1 + 4k^2 h^2}
 \end{aligned} \tag{11}$$

315 In Figure 3, we depict a random function with RMS 1% and exponential correlation (panels
 316 a and b), its power spectrum (d) and the predicted elastic attenuation (d). The result of the
 317 numerical simulation is in black, the analytical solution in red, the green lines average 50
 318 random realizations. The maximum of the predicted attenuation corresponds to a wavenum-
 319 ber $k = 1/(2h) = 0.083$ (wavelength $4\pi h \approx 75$ km) and reaches $\sigma^2/4 = 1.25 \times 10^{-5}$. Notice
 320 that this time, as the heterogeneities are localized in a restricted bandwidth, with the same
 321 RMS they lead to a 2.5 larger attenuation than when we assumed that the heterogeneities
 322 were distributed over 3.6 decades. Therefore a RMS small scale heterogeneity of 2.4-3.6 %
 323 would explain the observed P attenuation for periods around a few seconds. This is still
 324 much larger than what has been suggested for the lower mantle, but would be reasonable
 325 for upper mantle heterogeneities.

326 6. Conclusion

327 The short wavelength content of the mantle heterogeneities is mostly due to petrologi-
 328 cal anomalies multiply folded by convection and with a power spectrum decreasing as $1/k$.

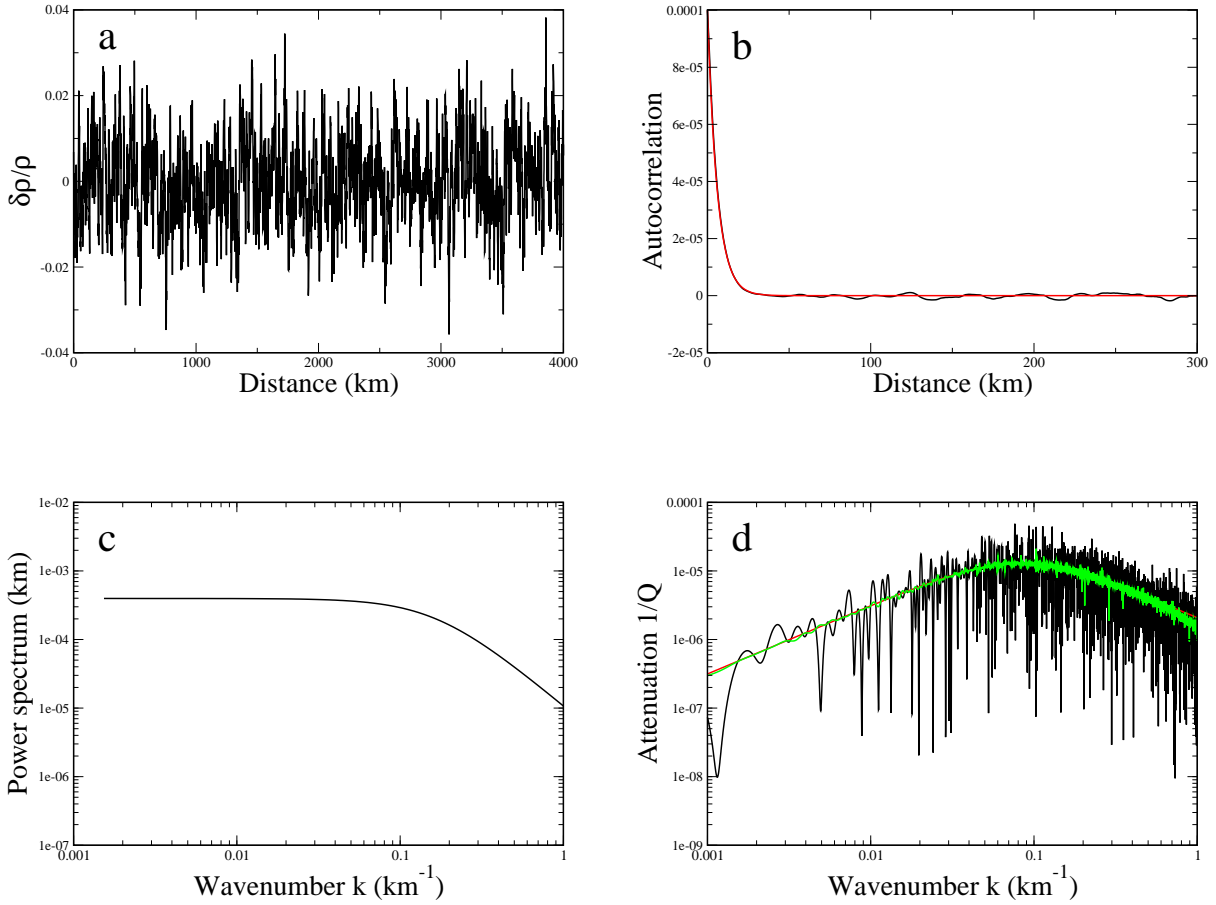


Figure 3: We generate a random density anomaly with 1% RMS amplitude (panel a) and exponential autocorrelation (panel b, computed autocorrelation in black, theoretical exponential autocorrelation with correlation length of 6 km in red). Its power spectrum is shown in panel (c). The computed (black) and theoretical (red) attenuations are depicted in panel (d). The green attenuation corresponds to the average of 50 random realizations similar to that of panel (a).

329 We present simple models of seismic waves traveling perpendicularly across a 1D laminated
 330 structure with this kind of spectrum and show that it results in multiple reflection and in
 331 the dispersion of a coherent signal into incoherent noise. The decrease in amplitude of the
 332 transmitted wave results in an apparent attenuation (elastic attenuation) that we compute,
 333 first, numerically and exactly, and second, using a simple approximated but analytical ex-
 334 pression. We show that the elastic attenuation is on average independent of the frequency.

335 This is true whether the density, the elasticity or the anisotropy (keeping uniform isotropic
336 elastic parameters) is the variable varying with a $1/k$ spectrum. When these quantities vary
337 together in an incoherent fashion, the elastic attenuations due to each variable, sum up. A
338 larger attenuation is obtained when these variables are correlated which is likely the case,
339 at least for density and the isotropic parameters. Similar results should remain valid for a
340 non-normal incidence.

341 In order to explain the whole attenuation of the mantle by elastic attenuation only and
342 over 3.6 decades of frequency, spatial variations in density and elastic parameters of the
343 order of 6-9 % are needed. Our model does not discuss the location of these heterogeneities,
344 in the shallow mantle or in the deep Earth. This remains large compared to what is seen in
345 tomography; a few % in the upper mantle, less than 1% in the lower mantle, but comparable
346 to the heterogeneity level of the lithosphere. If we reduce the range of frequencies over which
347 we explain the attenuation, we can decrease the amplitude of heterogeneities to levels similar
348 to those measured in laboratory between different compositions: eclogite/harzburgite have
349 density/elasticity differences in most of the mantle of 2 to 4% (Irifune and Ringwood, 1993;
350 Ricolleau et al., 2010). Even in this case, the amplitude of these small-scale heterogeneities
351 is much larger than what has been inferred in the deep mantle by previous studies (Margerin
352 and Nolet, 2003; Mancinelli and Shearer, 2013). In the inner core, a level of heterogeneity
353 of a few % between random patches has been invoked to explain the seismic observations
354 (Cormier, 2002; Calvet and Margerin, 2008).

355 There are many complexities that we have not taken into account. The P-SV conversions
356 provide another way to distribute the energy incoherently, and would probably increase the
357 apparent attenuation for the same spectrum of heterogeneities. The same would be true
358 when a general anisotropic elastic tensor is considered (while we have only considered transverse
359 anisotropy). It seems that all these complexities will also lead to a similar expression as (4),
360 and a constant attenuation for a medium stirred following Batchelor regime. The fact that
361 the heterogeneities are far from parallel as it has been considered here, should also be taken
362 into account. It seems it should further increase the elastic attenuation.

363 If most of Earth's attenuation is due to [small scale](#) heterogeneities with a $1/k$ spectrum and a

364 RMS of a few %, then the weak variation of attenuation with frequency would become easy to
365 explain. The fact that S waves are more attenuated than P waves would be simply related to
366 the fact that anisotropy gives S waves more degrees of freedom to disperse its elastic energy.
367 It would be misleading to interpret these Q_P and Q_S attenuations in term of Q_κ and Q_μ ,
368 as this would wrongly interpret a scattering phenomenon in terms of dissipation. The real
369 dissipative attenuation, that must be present, would be hidden by the elastic attenuation,
370 and the intrinsic quality factors Q_κ and Q_μ would simply be higher than what has been
371 observed. Their values might then respect the condition $3\kappa Q_\kappa^{-1} > 2\mu Q_\mu^{-1}$ and might not
372 imply a strange auxetic rheology for the mantle.

373 In principle, the modeling of coda waves could separate the intrinsic and scattering
374 effects (Shearer and Earle, 2004). If the amplitude of heterogeneities necessary to explain
375 the seismic attenuation by elastic scattering implies unrealistically large and complex codas,
376 then it would imply that intrinsic attenuation dominates a frequency independent elastic
377 attenuation. Direct simulation of wave propagation (e.g., within an exact numerical scheme,
378 Komatitsch and Vilotte, 1998) for a 3D structure including small scale heterogeneities, will
379 in a close future be able to model precisely the effect of elastic scattering but computing
380 elastic wave fields up to ≈ 1 Hz on a global scale will certainly be a challenge.

381 **Acknowledgments**

382 We thank V. Cormier for his very constructive review and P. Shearer for his meticulous
383 work as editor. This work has been supported by the ANR CMBmelt 10-BLAN-622 and
384 ANR SISMOglob 11-BLAN-SIMI5-6-016-01. J.P. Montagner thanks the Institut Universi-
385 taire de France and the training network QUEST.

386 Agranier A., J. Blichert-Toft, D. Graham, V. Debaille, P. Schiano and F. Albarède, 2005, The spectra of
387 isotopic heterogeneities along the mid-Atlantic Ridge, *Earth. Planet. Sci. Lett.*, **238**, 96-109.

388 Allègre, C.J. and D.L. Turcotte, 1986, Implications of a two-component marble-cake mantle, *Nature*, **323**,
389 123-127.

390 Antonsen T. M. Jr and E. Ott, 1991, Multifractal power spectra of passive scalars convected by chaotic fluid
391 flows, *Phys. Rev. A*, **44**, 851-857.

392 Backus, G.E., 1962, Long-wave elastic anisotropy produced by horizontal layering, *J. Geophys. Res.*, **67**,
393 4427-4440.

394 Batchelor, G. K., Small-scale variation of convected quantities like temperature in turbulent fluid Part 1.
395 General discussion and the case of small conductivity, 1959, *J. Fluid Mech.*, **238**, 96-109.

396 Calvet, M. and L. Margerin, 2008, Constraints on grain size and stable iron phases in the uppermost inner
397 core from multiple scattering modeling of seismic velocity and attenuation, *Earth Planet. Sci. Lett.*, **267**,
398 200-212, doi: 10.1016/j.epsl.2007.11.048.

399 Capdeville, Y. and J.J. Marigo, 2007, Second-order homogenization of the wave equation for non-periodic
400 layered media, *Geophys. J. Int.*, doi:10.1111/j.1365-246X.207.03462.x.

401 Chevrot S., J.P. Montagner and R. Snieder, 1998, The spectrum of tomographic Earth models, *Geophys. J.*
402 *Int.*, **133**, 783-788.

403 Choy G. L., V.F. and Cormier, 1986, Direct measurement of the mantle attenuation operator from broad-
404 band P-wave-forms and S-wave-forms, *J. Geophys. Res.*, **91**, 7326-7342.

405 Coltice, N. and Y. Ricard, 1999, Geochemical observations and one layer mantle convection, *Earth Planet.*
406 *Sci. Lett.*, **174**, 125-137.

407 Cormier, V.F., 1995, Time-domain modelling of PKIKP precursors for constraints on the heterogeneity in
408 the lowermost mantle, *Geophys. J. Int.*, **121**, 725-736.

409 Cormier, V.F. and X. Li, 2002, Frequency dependent attenuation in the inner core: Part II. A scattering
410 and fabric interpretation, *J. Geophys. Res.*, **107**, doi: 10.1029/2002JB1796.

411 Cormier, V.F., 2011, Seismic viscoelastic attenuation, In: Encyclopedia of Solid Earth Geophysics, H. Gupta
412 (ed.), pp. 1279-1290, doi: 10.1007/978-90-481-8702-7, Springer.

413 Dahlen, F.A., 1982, The effect of data windows on the estimation of free oscillation parameters, *Geophys.*
414 *J. Royal Astron. Soc.*, **69**, 537-549.

415 Debayle, E. and Y. Ricard, 2012, A global shear velocity model of the upper mantle from fundamental and
416 higher Rayleigh mode measurements, *J. Geophys. Res.*, **117**, B10308, doi:10.1029/2012JB009288.

417 Debayle, E. and Y. Ricard, 2013, Seismic observations of large-scale deformation at the bottom of fast-
418 moving plates, *Earth Planet. Sci. Lett.*, **376**, 165-177, doi: 10.1016/j.epsl.2013.06.025.

419 Durand S., J. Matas, S. Ford, Y. Ricard, B. Romanowicz and J.P. Montagner, 2013, Insights from

420 ScS-S measurements on deep mantle attenuation, *Earth Planet. Sci. Lett.*, **374**, 101-110, doi:
421 10.1016/j.epsl.2013.05.026.

422 Faul, U.H. and I. Jackson, 2005, The seismological signature of temperature and grain size variations in the
423 upper mantle, *Earth Planet. Sci. Lett.*, **234**, 119-134.

424 Fichtner, A., B.L.N. Kennett and J. Trampert, 2013, Separating intrinsic and apparent anisotropy, *Phys.*
425 *Earth. Planet. Inter.*, **219**, 119-134, doi: 10.1016/j.pepi.2013.03.006.

426 Gurnis, M., 1986, Quantitative bounds on the size spectrum of isotopic heterogeneity within the mantle,
427 *Nature*, **323**, 317-320.

428 Hedlin, M. A. H., P. M. Shearer and P. S. Earle, 1997, Seismic evidence for small-scale heterogeneity through-
429 out the Earth's mantle, *Nature*, **387**, 145-150.

430 Hwang, Y.K. and J. Ritsema, 2011, Radial Q_μ structure of the lower mantle from teleseismic body-wave
431 spectra, *Earth Planet. Sci. Lett.*, **303**, 369-375.

432 Irifune, T. and A. Ringwood, 1993, Phase transformations in subducted oceanic crust and buoyancy rela-
433 tionships at depths of 600-800 km in the mantle, *Earth Planet. Sci. Lett.*, **117**, 101-110.

434 Jackson D. D. and D.L. Anderson, 1970, Physical mechanisms of seismic-wave attenuation, *Rev Geophys.*
435 *Space Phys.*, **8**, doi: 10.1029/RG008i001p00001.

436 Jackson, I., J. D. Fitz Gerald, U. H. Faul and B.H. Tan, 2002, Grain-size-sensitive seismic wave attenuation
437 in polycrystalline olivine *J. Geophys. Res.*, **107**, doi:10.1029/2001JB001225.

438 Jackson, I., 2007, Physical Origins of Anelasticity and Attenuation in Rock In Schubert (Ed.) *Treatise of*
439 *Geophysics*, Elsevier, pp. 493-525.

440 Kaelin, B. and L.R. Johnson, 1998, Dynamic composite elastic medium theory. Part I. One-dimensional
441 media *J. App. Phys.*, **84**, 5451-5457, doi: 10.1063/1.368307.

442 Kawakatsu, H., P. Kumar, Y. Takei, M. Shinohara, T. Kanazawa, E. Araki and K. Suyehiro, 2011, Seis-
443 mic Evidence for Sharp Lithosphere-Asthenosphere Boundaries of Oceanic Plates, *Science*, **324**, doi:
444 10.1126/science.1169499.

445 Knopoff, L., 1964, Q, *Rev. Geophys.*, **2**, 625-660.

446 Komatitsch, D. and J.P. Vilotte, 1998, The spectral element method: An efficient tool to simulate the
447 seismic response of 2D and 3D geological structures, *Bull. Seism. Soc. Am.*, **88**, 368-392.

448 Lekic, V., J. Matas J., M. Panning and B. Romanowicz, 2009, Measurements and implications of frequency
449 dependence of attenuation, *Earth Planet. Sci. Lett.*, **282**, 285-293

450 Liu, H. P., D.L. Anderson and H. Kanamori, 1976, Velocity dispersion due to anelasticity: implication for
451 seismology and mantle composition, *Geophys. J. Roy. Astron. Soc.*, **47**, 41-58.

452 Mancinelli, N. J. and P. M. Shearer, 2013, Reconciling discrepancies among estimates of small-scale mantle
453 heterogeneity from PKP precursors *Geophys. J. Int.*, **195**, 1721-1729.

454 Margerin L. and G. Nolet, 2003, Multiple scattering of high-frequency seismic waves in deep Earth: PKP
455 precursor analysis and inversion for mantle granularity, *J. Geophys. Res.*, **108**, doi:10.1029/2003JB002455.

456 Montagner, J-P., 1994, Can seismology tell us anything about convection in the mantle?, *Rev. Geophys.*,
457 **32**, 115-137.

458 Montagner, J-P. and L. Guillot, 2002, Seismic anisotropy and global geodynamics, *Reviews in Mineralogy
459 and Geochemistry*, **51**, 353-385, doi:10.2138/gsrmg.51.1.353.

460 Morozov I., 2013, http://seisweb.usask.ca/ibm/papers/Q/Morozov_bulk_and_shear_dissipation.

461 O'Doherty, R.F. and N.A. Anstey, 1971, Reflections on amplitudes, *Geophys. Prosp.*, **19**, 430-458.

462 Olson P., D.A. Yuen and D. Balsiger, 1984, Mixing of passive heterogeneities by mantle convection, *J.
463 Geophys. Res.*, **89**, 425-436.

464 Ricard, Y., E. Mattern and J. Matas, 2005, Synthetic tomographic images of slabs from mineral physics,
465 in VanDerHilst, RD; Bass, JD; Matas, J; et al. (Eds) Earth's deep mantle: structure, composition and
466 evolution, Geophysical Monograph Series, **160**, 283-300, doi: 10.1029/160GM17.

467 Ricard, Y, H.C. Nataf and J.P. Montagner, 1996, The three-dimensional seismological model a priori con-
468 strained: Confrontation with seismic data, *J. Geophys. Res.*, **101**, 8457-8472, doi: 10.1029/95JB03744.

469 Ricolleau, A, J.P. Perrillat, G. Fiquet, I. Daniel, J. Matas, A. Addad, N. Menguy, H. Cardon, M. Mezouar
470 and N. Guignot, 2010, Phase relations and equation of state of a natural MORB: Implications for
471 the density profile of subducted oceanic crust in the Earth's lower mantle *J. Geophys. Res.*, **115**, doi:
472 10.1029/2009JB006709

473 Romanowicz B. and B. Mitchell, 2006, Deep Earth structure - Q in the Earth from crust to core, In Schubert
474 (Ed.) *Treatise of Geophysics*, Elsevier, pp. 731-774.

475 Schmandt, B., K. Dueker, S. Hansen, J. Jaszbinsek and Z. Zhang, 2011, A sporadic low-velocity layer atop
476 the western U.S. mantle transition zone and short-wavelength variations in transition zone discontinuities,
477 *Geochem. Geophys. Geosys.*, **12**, 1-26.

478 Shapiro, S. A., P. Hubral and B. Ursin, 1996, Reflectivity/transmissivity for one-dimensional inhomogeneous
479 random elastic media: dynamic-equivalent-medium approach, *Geophys. J. Int.*, **126**, 194-196.

480 Shearer, P.M. and P.S. Earle, 2008, Observing and modeling elastic scattering in the deep Earth, In *Advances
481 in Geophysics*, **50**, 167-193, doi: 10.1016/S0065-2687(08)00006-X.

482 Shearer, P.M. and P.S. Earle, 2004, The global short-period wavefield modelled with a Monte Carlo seismic
483 phonon method, *Geophys. J. Int.*, **158**, 1103-1117, doi: 10.1111/j.1365-246X.2004.02378.x.

484 Shito, A., S.I. Karato and J. Park, 2004, Frequency dependence of Q in Earth's upper mantle inferred from
485 continuous spectra of body wave, **31**, L12603, doi: 10.1029/2004GL019582.

486 Tauzin, B., E. Debayle, and G. Wittlinger, 2010, Seismic evidence for a global low velocity layer within the
487 Earth's upper mantle, *Nature Geoscience*, **3**, 718-721.

488 Wang, N., J.P. Montagner, A. Fichtner and Y. Capdeville, 2013, Intrinsic versus extrinsic seismic anisotropy:
489 The radial anisotropy in reference Earth models, *Geophysical Research Letters*, **40**, 4284-4288.
490 Waters, K.R., J. Mobley and J.G. Miller, 2005, Causality-imposed (Kramers-Kronig) relationships between
491 attenuation and dispersion, *IEEE Transactions On Ultrasonics Ferroelectrics And Frequency Control*, **52**,
492 822-833, doi: 10.1109/TUFFC.2005.1503968.

493 **A. Propagation of a S wave perpendicular to a stratified isotropic medium**

494 The wave equation for a S wave propagating along z , perpendicularly to a layered struc-
495 ture writes

$$\rho \frac{\partial^2 u_x}{\partial t^2} = \frac{\partial \sigma_{xz}}{\partial z} \quad (\text{A.1})$$

496 where u_x is the displacement component along ox and σ_{xz} the stress component. For a
497 periodic wave of angular frequency ω all variables also depend implicitly on time with terms
498 in $\exp(-i\omega t)$, and using Hooke's law, we can recast this second order equation as a first
499 order differential system

$$\frac{d}{dz} \begin{pmatrix} u_x \\ \sigma_{xz}/(\rho_0\omega v_0) \end{pmatrix} = k_0 M \begin{pmatrix} u_x \\ \sigma_{xz}/(\rho_0\omega v_0) \end{pmatrix}, \quad (\text{A.2})$$

500 where ρ_0 and v_0 are some characteristic uniform density and velocity, $k_0 = \omega/v_0$, and where
501 the matrix M is

$$M = -\frac{\rho}{\rho_0} \begin{pmatrix} 0 & 0 \\ 1 & 0 \end{pmatrix} + \frac{\rho_0 v_0^2}{\mu} \begin{pmatrix} 0 & 1 \\ 0 & 0 \end{pmatrix} \quad (\text{A.3})$$

502 In an homogeneous medium, the matrix M becomes the uniform matrix M_0 which de-
503 scribes the wavefield in a homogeneous medium

$$M_0 = \begin{pmatrix} 0 & 1 \\ -1 & 0 \end{pmatrix}. \quad (\text{A.4})$$

504 The diagonalization of the matrix M_0 shows that its eigenvalues are i and $-i$ and its eigen-
505 vectors can be taken as the columns of the matrix V

$$V = \begin{pmatrix} 1 & 1 \\ i & -i \end{pmatrix}. \quad (\text{A.5})$$

506 In a homogeneous medium, the system (A.2) thus describes a S wave propagating in one
507 direction (wavenumber ik_0), and another in the opposite direction (wavenumber $-ik_0$). In
508 a heterogeneous medium, the density ρ , and the rigidity μ present in A.3 are function of

509 z . Let us consider the propagation in the reference frame appropriate in the absence of
 510 perturbations by using the vector $g = V^{-1}(u_x, \sigma_{xz}/(\rho_0\omega v_0))^t$. It verifies

$$\frac{dg}{dz} = k_0 V^{-1} M V g = i k_0 L g. \quad (\text{A.6})$$

511 The 2x2 matrix $L = V^{-1} M V$ can be re-written as

$$L = \begin{pmatrix} M_1 & M_2 \\ -M_2 & -M_1 \end{pmatrix}, \quad (\text{A.7})$$

512 where

$$\begin{aligned} M_1 &= 1 + \frac{1}{2} A = 1 + \frac{1}{2} \left(\frac{\delta\rho}{\rho_0} - \frac{\delta\mu}{\mu} \right), \\ M_2 &= \frac{1}{2} C = \frac{1}{2} \left(\frac{\delta\rho}{\rho_0} + \frac{\delta\mu}{\mu} \right), \\ \frac{\delta\rho}{\rho_0} &= \frac{\rho - \rho_0}{\rho_0} \quad \text{and} \quad \frac{\delta\mu}{\mu} = \frac{\mu - \mu_0}{\mu} = \frac{1/\mu_0 - 1/\mu}{1/\mu_0} \end{aligned} \quad (\text{A.8})$$

513 The matrix L becomes indeed diagonal in a homogeneous medium. Eq. (A.6) describes the
 514 propagation of a down- and an up-going S wave of amplitudes denoted S_{dy}, S_{uy} . As this
 515 differential system is linear, there exists a 2X2 propagator P relating the waves amplitudes
 516 at z , to their amplitudes at $z = 0$ such that

$$(S_{dx}(z), S_{ux}(z))^t = P(0, z) (S_{dx}(0), S_{ux}(0))^t. \quad (\text{A.9})$$

517 This propagator also verifies eq. (A.6) so that

$$\frac{dP}{dz} = i k_0 L P. \quad (\text{A.10})$$

518 P contains 4 coefficients that can be interpreted as combinations of the reflection and trans-
 519 mission matrices of incident waves going down R_d, T_d , or up, R_u, T_u . For example an up
 520 going wave incident at z , is partially refracted as a down going wave with the amplitude
 521 $(S_{dx}(z), S_{ux}(z))^t = R_u(S_{ux}(z), S_{ux}(z))^t$ and partly transmitted at $z = 0$ with the amplitude
 522 $(S_{ux}(0), S_{ux}(0))^t = T_u(S_{ux}(z), S_{ux}(z))^t$ while $(S_{dx}(0), S_{dx}(0))^t = 0$ (we kept the notation con-
 523 ventions of Shapiro et al. (1996)). Comparing these definitions with that of the propagator

524 (A.9), proves that the rightside column of P is just $R_u T_u^{-1}$ and T_u^{-1} . Similarly, by consider-
 525 ing an incident up going wave at $z = 0$ we conclude that the matrix P can be interpreted
 526 as

$$P = \begin{pmatrix} T_d - R_u T_u^{-1} R_d & R_u T_u^{-1} \\ -T_u^{-1} R_d & T_u^{-1} \end{pmatrix}. \quad (\text{A.11})$$

527 Substituting eq. (A.11) into (A.10) we find the system of differential equations

$$\begin{cases} \frac{dR_u}{dz} = ik_0(M_2 + M_1 R_u + R_u M_1 + R_u M_2 R_u) \\ \frac{dT_u}{dz} = ik_0(T_u M_1 + T_u M_2 R_u) \\ \frac{dT_d}{dz} = ik_0(M_1 T_d + R_u M_2 T_d) \\ \frac{dR_d}{dz} = ik_0(T_u M_2 T_d) \end{cases}. \quad (\text{A.12})$$

528 This is a system of 4 differential equations to be solved (in the case we are dealing with,
 529 all the terms M_1 , M_2 , R_u , T_u are scalars and, e.g., $M_1 R_u + R_u M_1 = 2M_1 R_u$. Later (see
 530 supplementary material C), these terms will become matrices and for more generality we
 531 keep this writing which works for matrices (see Shapiro et al., 1996)). Solving numerically
 532 this differential system leads exactly to the various transmission and reflection coefficients.
 533 The two first equations can be separately integrated from 0 with the initial conditions
 534 $R_u(0) = 0$ and $T_u(0) = 1$ and give identical results than a Thomson-Haskell integration.
 535 The formalism that we used to derive (A.12) is however very useful as it has allowed us to
 536 set up the problem in the form of a differential form for which classic analytical tools can
 537 found approximative solutions.

538 To do so we consider that A , C , $\delta\rho/\rho_0$ and $\delta\mu/\mu$ are small quantities and then solve
 539 equations (A.12) at various orders. We only consider up going propagation and we only need
 540 to solve the first two equations of (A.12) to find R_u and T_u , that from now on we will simply
 541 write R and T . We can therefore write $T = T^{(0)} + T^{(1)} + T^{(2)} + \dots$ and $R = R^{(1)} + R^{(2)} + \dots$
 542 where $T^{(n)}$ and $R^{(n)}$ are of order n in the small quantities A and C . Introducing these
 543 expansions into equations (A.12) and focussing on T , we get at order (0), (1) and (2)

$$\begin{cases} T^{(0)} = \exp(ik_0 z) \\ T^{(1)} = \frac{ik_0}{2} \exp(ik_0 z) \int_0^z A(u) du \\ T^{(2)} = -\frac{k_0^2}{4} \exp(ik_0 z) \left[\int_0^z \int_0^u A(u) A(v) dudv + \int_0^z \int_0^u C(u) C(v) e^{2ik_0(u-v)} dudv \right] \end{cases} \quad (\text{A.13})$$

544 Similar expressions could also be obtained for the other components of the transmission and
545 reflection matrices. The transmission coefficient T , including all the terms up to the second
546 order in elastic perturbations is thus $T^{(0)} + T^{(1)} + T^{(2)}$. Noticing that $\int_0^z \int_0^u A(u)A(v)dudv =$
547 $1/2 \left(\int_0^z A(u)du\right)^2$ (the two expressions have the same z -derivatives and are equal for $z = 0$)
548 and using the expansion of the exponential up to second order, we see that T correct up to
549 second order can be written as

$$T = \exp \left[ik_0 z + \frac{1}{2} ik_0 \int_0^z A(u)du - \frac{k_0^2}{4} \int_0^z \int_0^u C(u)C(v)e^{2ik_0(u-v)} dudv \right]. \quad (\text{A.14})$$

550 The term at 1^{st} order is imaginary and just affects the phase, at 2^{nd} order amplitude and
551 phase are perturbed.

552 The transmission coefficient (A.14) is of the form $T = \exp(iKz)$ where K is a complex
553 wavenumber. The heterogeneity of the medium, by scattering energy and by making the
554 direct wave loose coherency, is therefore formally equivalent to an attenuating and dispersive
555 medium. We can express the apparent wave number K as

$$K = k_0 + \frac{k_0}{2z} \int_0^z A(u) du + i \frac{k_0^2}{4z} \int_0^z \int_0^u C(u)C(v)e^{2ik_0(u-v)} dudv \quad (\text{A.15})$$

556 The perturbation at first order cancels when $A = \delta\rho/\rho_0 - \delta\mu/\mu = \delta\rho/\rho_0 + \delta(1/\mu)/(1/\mu_0)$
557 is properly chosen to have a zero average (i.e., $\int_0^z A(u)du = 0$) which means that the average
558 density and the average inverse rigidity are both zero (or that v_0 is the average velocity). To
559 simplify the integral present in this expression, let us call $F(k_0)$:

$$F(k_0) = \int_0^z C(u) \left(\int_0^u C(v)e^{2ik_0(u-v)} dv \right) du, \quad (\text{A.16})$$

560 so that the apparent wave number is

$$K = k_0 + i \frac{k_0^2}{4z} F(k_0). \quad (\text{A.17})$$

561 The imaginary part of $F(k_0)$ involves a sine, while the real part, $G(k_0) = \text{Re}(F(k_0))$,
562 involves a cosine; they are therefore related by a Hilbert transform. One has $\text{Im}(F(k_0)) =$
563 $-\mathcal{H}[G(k_0)]$ where \mathcal{H} denotes the Hilbert transform, and

$$K = k_0 + \frac{k_0^2}{4z} \mathcal{H}[G(k_0)] + i \frac{k_0^2}{4z} G(k_0). \quad (\text{A.18})$$

564 This expression is a general consequence of the Kramers-Kronig relations that relate in a
 565 general way, attenuation and dispersion (e.g., Waters et al., 2005). Writing $K = k + ik_0/2Q$,
 566 where k and Q are real numbers, the resulting medium is attenuating with

$$\frac{1}{Q} = \frac{k_0 G(k_0)}{2z} \quad (\text{A.19})$$

567 and dispersive with

$$k = k_0 + \frac{k_0^2}{4z} \mathcal{H}[G(k_0)]. \quad (\text{A.20})$$

568 To compute $G(k_0) = \text{Re}(F(k_0))$, we change the order of the integrations in the expression
 569 of $F(k_0)$

$$F(k_0) = \int_0^z C(v) \left(\int_v^z C(u) e^{2ik_0(u-v)} du \right) dv. \quad (\text{A.21})$$

570 Now by swapping the names of the variables u and v ,

$$F(k_0) = \int_0^z C(u) \left(\int_u^z C(v) e^{-2ik_0(u-v)} dv \right) du. \quad (\text{A.22})$$

571 Therefore, using F^* for the conjugate of F , adding the conjugate of (A.16) with (A.22), we
 572 get

$$\begin{aligned} 2G(k_0) &= F(k_0) + F^*(k_0) \\ &= \int_0^z \int_0^z C(u) C(v) e^{-2ik_0(u-v)} du dv \\ &= \int_0^z C(u) e^{-2ik_0 u} du \int_0^z C(v) e^{2ik_0 v} dv \\ &= \left| \int_0^z C(u) e^{-2ik_0 u} du \right|^2 \end{aligned} \quad (\text{A.23})$$

573 For a stationary signal f , the power spectrum is defined as

$$S_C(k_0) = \lim_{z \rightarrow +\infty} \frac{1}{z\sqrt{2\pi}} \left| \int_0^z C(u) e^{-ik_0 u} du \right|^2 \quad (\text{A.24})$$

574 (notice that other definitions of the spectrum exist and may introduce different constants in
 575 the expressions that follow). According to (A.23), $G(k_0)$ is related to the power spectrum
 576 of C by

$$2G(k_0) \approx z\sqrt{2\pi} S_C(2k_0). \quad (\text{A.25})$$

577 We therefore simplify (A.19) that becomes

$$\frac{1}{Q} = \frac{\sqrt{2\pi}}{4} k_0 S_C(2k_0), \quad (\text{A.26})$$

578 i.e., the apparent attenuation is simply related to the power spectrum of C defined in (A.8)
 579 that contains the heterogeneities in density and rigidity. This is the main result that we use
 580 in this paper.

581 A function can also be characterized by its autocorrelation instead of by its Fourier power
 582 spectrum. The autocorrelation of a stationary signal is

$$R_C(x) = \lim_{z \rightarrow +\infty} \frac{1}{z} \int_0^z C(u+x)C(u)du \quad (\text{A.27})$$

583 The Wiener-Khinchin theorem states that the autocorrelation function R_C and the power
 584 spectral density S_C are simply related by

$$\begin{aligned} R_C(x) &= \frac{1}{\sqrt{2\pi}} \int_{-\infty}^{\infty} S_C(k) e^{ikx} dk \\ S_C(k) &= \frac{1}{\sqrt{2\pi}} \int_{-\infty}^{\infty} R_C(x) e^{-ikx} dx \end{aligned} \quad (\text{A.28})$$

585 The elastic attenuation can therefore be written as

$$\frac{1}{Q} = \frac{1}{4} k_0 \int_{-\infty}^{+\infty} R_C(x) e^{-2ik_0x} dx, \quad (\text{A.29})$$

586 **B. Propagation of a P wave perpendicular to a stratified isotropic medium**

587 Although the algebra was quite long in supplementary material (A), the generalization
 588 to other cases is now very simple. The wave equation for a P wave propagating along z ,
 589 perpendicularly to a layered structure writes

$$\rho \frac{\partial^2 u_z}{\partial t^2} = \frac{\partial \sigma_{zz}}{\partial z} \quad (\text{B.1})$$

590 that we can recast as a first order differential system. This system can then be diagonalized,
 591 the equations rewritten in such a way to make explicit the homogeneous system and the

592 perturbations. The matrix L (see (A.6)) can again be written in the form (A.7) where the
 593 coefficients M_1 and M_2 (see (A.8)) are now

$$\begin{aligned} M_1 &= 1 + \frac{1}{2}A = 1 + \frac{1}{2} \left(\frac{\delta\rho}{\rho_0} - \frac{\delta(K + 4/3\mu)}{K + 4/3\mu} \right) \\ M_2 &= \frac{1}{2}C = \frac{1}{2} \left(\frac{\delta\rho}{\rho_0} + \frac{\delta(K + 4/3\mu)}{K + 4/3\mu} \right) \end{aligned} \quad (\text{B.2})$$

594 Therefore, except that instead of rigidity it is now $K + 4/3\mu$ that appears, the equations are
 595 similar to (A.8) and of course we also get

$$\frac{1}{Q} = \frac{\sqrt{2\pi}}{4} k_0 S_C(2k_0), \quad (\text{B.3})$$

596 where C contains now the density and the $K + 4/3\mu$ perturbations.

597 **C. Propagation of a S wave perpendicular to a stratified transverse anisotropic** 598 **medium**

599 We can briefly discuss the case of transverse anisotropy (anisotropy in the xy plane with
 600 an angle $\psi(z)$ with the x -axis), as the method remains close to that discussed in supplemen-
 601 tary material A. The wave equation for a S wave propagating along z , perpendicularly to a
 602 layered structure writes

$$\rho \frac{\partial^2}{\partial t^2} \begin{pmatrix} u_x \\ u_y \end{pmatrix} = \frac{\partial}{\partial z} \begin{pmatrix} \sigma_{xz} \\ \sigma_{yz} \end{pmatrix} \quad (\text{C.1})$$

603 where u_x and u_y are the displacement components and σ_{xz} and σ_{yz} the stress components,
 604 all quantities being now coupled by anisotropy. For a periodic wave of angular frequency ω
 605 and using Hooke's law accounting for transverse anisotropy, we can recast this second order
 606 equation under the form of a first order differential system

$$\frac{d}{dz} \begin{pmatrix} u_x \\ u_y \\ \sigma_{xz}/(\rho_0\omega v_0) \\ \sigma_{yz}/(\rho_0\omega v_0) \end{pmatrix} = k_0 M \begin{pmatrix} u_x \\ u_y \\ \sigma_{xz}/(\rho_0\omega v_0) \\ \sigma_{yz}/(\rho_0\omega v_0) \end{pmatrix}, \quad (\text{C.2})$$

607 where ρ_0 and v_0 are some characteristic density and velocity, $k_0 = \omega/v_0$, and where the
 608 matrix M is

$$M = -\frac{\rho}{\rho_0} \begin{pmatrix} 0 & 0 & 0 & 0 \\ 0 & 0 & 0 & 0 \\ 1 & 0 & 0 & 0 \\ 0 & 1 & 0 & 0 \end{pmatrix} + \rho_0 v_0^2 \frac{L+N}{2LN} \begin{pmatrix} 0 & 0 & 1 & 0 \\ 0 & 0 & 0 & 1 \\ 0 & 0 & 0 & 0 \\ 0 & 0 & 0 & 0 \end{pmatrix} +$$

(C.3)

$$\rho_0 v_0^2 \frac{N-L}{2LN} \begin{pmatrix} 0 & 0 & \cos 2\psi & \sin 2\psi \\ 0 & 0 & \sin 2\psi & -\cos 2\psi \\ 0 & 0 & 0 & 0 \\ 0 & 0 & 0 & 0 \end{pmatrix}.$$

609 The density ρ , the maximum and minimum elastic constants L , N as well as the direction
 610 of anisotropy ψ are functions of z . After rotation in the appropriate reference frame, we
 611 transform (C.2) into an equation similar to (A.6) but where the L matrix is now 4x4 and
 612 can be re-written in terms of two 2x2 symmetric matrices, M_1 et M_2 (Shapiro et al., 1996)

$$L = \begin{pmatrix} M_1 & M_2 \\ -M_2 & -M_1 \end{pmatrix},$$

(C.4)

613 that can be expressed from the 2x2 identity matrix Id and from the matrix J

$$J = \begin{pmatrix} \cos(2\psi) & \sin(2\psi) \\ \sin(2\psi) & -\cos(2\psi) \end{pmatrix}$$

(C.5)

614 by

$$M_1 = Id + \frac{1}{2} \left(\frac{\delta\rho}{\rho_0} - \frac{\delta\mu}{\mu} \right) Id + \frac{1}{2} \frac{\delta a}{\mu} J$$

$$M_2 = \frac{1}{2} \left(\frac{\delta\rho}{\rho_0} + \frac{\delta\mu}{\mu} \right) Id + \frac{1}{2} \frac{\delta a}{\mu} J$$

(C.6)

615 which are in agreement with (A.8) in the absence of anisotropy and where $\delta\rho/\rho_0 = (\rho -$
 616 $\rho_0)/\rho_0$, $\delta\mu/\mu = (2LN - \rho_0 v_0^2(L+N))/(2LN)$ and $\delta a/\mu = \rho_0 v_0^2(N-L)/(2LN)$. In the

617 following we will also use the different terms of these matrices that we name A , B , C , D
 618 and M with

$$\begin{aligned}
 M_1 &= Id + \frac{1}{2} \begin{pmatrix} A & M \\ M & B \end{pmatrix} \\
 M_2 &= \frac{1}{2} \begin{pmatrix} C & M \\ M & D \end{pmatrix}
 \end{aligned}
 \tag{C.7}$$

619 and two of these terms will specifically appear in our final results

$$\begin{aligned}
 C &= \frac{\delta\mu}{\mu} + \frac{\delta\rho}{\rho_0} + \cos(2\psi) \frac{\delta a}{\mu} \\
 M &= \sin(2\psi) \frac{\delta a}{\mu}.
 \end{aligned}
 \tag{C.8}$$

620 We have therefore succeeded in writing the wave propagation equations as a differential sys-
 621 tem where the perturbations of density, velocity and anisotropy are explicit. The reflection
 622 and transmission matrices are verifying the same equations (A.12) that can be approximately
 623 solved by Taylor expansion to get the apparent quality factor Q as

$$\frac{1}{Q} = \frac{k_0}{2z} \int_0^z \int_0^u (M(u)M(v) + C(u)C(v)) \cos[2k_0(u-v)] dudv.
 \tag{C.9}$$

624 which can be expressed as a function of the spectra of C and M as

$$\frac{1}{Q} = \frac{\sqrt{2\pi}}{4} k_0 (S_M(2k_0) + S_C(2k_0)),
 \tag{C.10}$$

625 expression equivalent to (A.26) in the absence of anisotropy ($\delta a \propto L - N = 0$).

626 D. Propagation of a S-H wave in a stratified medium

627 This time, we assume that the displacement is along y and the incidence to the lam-
 628 inations defined by the angle to the normal θ . All the variables depend implicitly of
 629 $\exp(i(k_0 x \sin \theta - \omega t))$ and the amplitudes of the displacement and shear stress are func-
 630 tion of z only, and are solutions of

$$\frac{d}{dz} \begin{pmatrix} u_y \\ \sigma_{yz}/(\rho_0 \omega v_0) \end{pmatrix} = k_0 M \begin{pmatrix} u_y \\ \sigma_{yz}/(\rho_0 \omega v_0) \end{pmatrix},
 \tag{D.1}$$

631 where the matrix M is given by

$$M = -\frac{\rho}{\rho_0} \begin{pmatrix} 0 & 0 \\ 1 & 0 \end{pmatrix} + \frac{\rho_0 v_0^2}{\mu} \begin{pmatrix} 0 & 1 \\ 0 & 0 \end{pmatrix} + \frac{\mu}{\rho_0 v_0^2} \begin{pmatrix} 0 & 0 \\ \sin^2 \theta & 0 \end{pmatrix}. \quad (\text{D.2})$$

632 Only the last term differs from the case of a normal incidence (compare with (A.3)). Follow-
 633 ing exactly the same approach as in supplementary material (A) we end up with the same
 634 equation (A.6), where the matrix L (A.7) depends now of the coefficients

$$\begin{aligned} M_1 &= \cos \theta + \frac{1}{2} A \\ M_2 &= \frac{1}{2} C \end{aligned} \quad (\text{D.3})$$

635 where

$$\begin{aligned} A &= \frac{1}{\cos \theta} \left(\frac{\delta \rho}{\rho_0} - \frac{\delta \mu}{\mu_0} \right) + 2 \cos \theta \left(\frac{\delta \mu}{\mu_0} \right)^2 \\ C &= \frac{1}{\cos \theta} \frac{\delta \rho}{\rho_0} + \frac{\cos(2\theta)}{\cos \theta} \frac{\delta \mu}{\mu_0} - 2 \cos \theta \left(\frac{\delta \mu}{\mu_0} \right)^2 \end{aligned} \quad (\text{D.4})$$

636 (as μ appears both in a numerator and in a denominator in (D.2), we use the variable $\delta\mu/\mu_0$
 637 in this case while in the other cases it was simpler to consider $\delta\mu/\mu$, see (A.8), two quantities
 638 that only differ at second order). The A and C terms are in agreement to the case with
 639 normal incidence when $\theta = 0$ (see (A.8)). Solving the propagation at second order gives
 640 finally

$$T = \exp \left(i(k_0(x \sin \theta + z \cos \theta) - \omega t) - z \frac{\sqrt{2\pi}}{4} S_C(2k_0 \cos \theta) \right) \quad (\text{D.5})$$

641 Calling l the distance along the ray ($x = l \sin \theta$ and $z = l \cos \theta$), the transmitted amplitude
 642 is therefore

$$T = \exp \left(i(k_0 l - \omega t) - l \cos \theta \frac{\sqrt{2\pi}}{4} S_C(2k_0 \cos \theta) \right) \quad (\text{D.6})$$

643 and the equivalent attenuation (in agreement with the previous estimate when $\theta = 0$,
 644 (A.26)), is therefore

$$\frac{1}{Q} = \frac{\sqrt{2\pi} \cos \theta}{4} k_0 S_C(2k_0 \cos \theta), \quad (\text{D.7})$$

645 where θ is also present in the definition of C . Three cases are easy to describe. When
 646 $\delta\mu/\mu_0 = 0$ and for a spectrum in $1/k$, we simply replace $S_C(2k_0 \cos \theta)$ by $S_C(2k_0)/\cos \theta =$

647 $S_\rho(2k_0)/\cos^3\theta$ where S_ρ is the density spectrum to obtain

$$\frac{1}{Q} = \frac{\sqrt{2\pi}}{4\cos^2\theta} k_0 S_\rho(2k_0). \quad (\text{D.8})$$

648 When $\delta\rho/\rho_0 = 0$, $S_C(2k_0 \cos\theta) = S_\mu(2k_0) \cos^2(2\theta)/\cos^3\theta$ where S_μ is the rigidity spectrum

$$\frac{1}{Q} = \frac{\sqrt{2\pi} \cos^2(2\theta)}{4\cos^2\theta} k_0 S_\mu(2k_0). \quad (\text{D.9})$$

649 When $\delta\rho/\rho_0 = \delta\mu/\mu_0$,

$$\frac{1}{Q} = \sqrt{2\pi} k_0 S_\rho(2k_0). \quad (\text{D.10})$$

650 Notice that this expression is in agreement with what was obtained for a normal incidence
651 (A.26). The absence of a factor 4 (compare (D.10) and (A.26)) is simply due to the fact
652 that this last expression assumes a perfect correlation between density and rigidity.